ELSEVIER

Polymer 43 (2002) 149–157

polymer

www.elsevier.com/locate/polymer

Development of structural hierarchy during uniaxial drawing of PEEK/PEI blends from amorphous precursors

S. Bicakci, M. Cakmak*

College of Polymer Engineering & Polymer Science, Polymer Engineering Institute, University of Akron, Akron, OH 44325-0301, USA

Received 19 March 2001; received in revised form 20 August 2001; accepted 22 August 2001

Abstract

When poly(ether ether ketone)/poly(ether imide) (PEEK/PEI) blends are drawn in their rubbery region, prior to the critical draw ratio, they remain amorphous. Subsequent to the onset of strain hardening, the stress rises rapidly as a result of strain-induced crystallization of the chains highly oriented in the direction of strain. It is during this stage of deformation process that *a highly structured physical network is formed where oriented crystallites act as nodes in the network structure*. The wide angle X-ray scattering data indicate that chains in these 'nodes' are highly oriented and the three dimensional crystalline lattice is not well established due to poor axial registry of these highly oriented chains. This is evidenced by the absence of off-equatorial peaks. During this period, the effectiveness of drawing arises from the existence of the tie chains aligned in the direction of draw and forming the net between the crystallites. PEI, though a stiff and bulky chain, is found to delay the oriented crystallization rate of PEEK, but has little effect on its crystalline orientation in the composition range investigated.

Keywords: Crystallites; Thermoplastic films; PEEK

1. Introduction

Blends of poly(ether ether ketone) (PEEK) with poly(ether imide) (PEI) combine the useful properties of each of the components such as the excellent mechanical properties, good solvent resistance and very high use temperature of PEEK [1], with the very high glass transition of PEI. This specific blend of materials is also an attractive system from a scientific perspective for understanding the morphology of binary blends with a crystallizable component (PEEK) and a noncrystallizable component (PEI).

Miscibility of these blends [2–9] and their quiescent crystallization [3–5,10–15] in the melt and the rubbery region have been extensively studied. However, there has been little scientific effort expended on the study of their deformation and the resulting crystallization behavior. As most polymer processes and polymer applications involve stretching and subsequent annealing, it is of significant interest to study the development of strain induced structure and its hierarchy. The study of deformation becomes much more complex for studies involving the blends of macromolecules, contrary to homopolymers. Most of the literature on the orientation and relaxation of uniaxially drawn miscible blends includes materials with amorphous components [16–20]. It was shown that although these blends are miscible as a result of specific interactions between the components, when subjected to uniaxial deformation, the individual components can show different orientation behaviors as demonstrated in a study done on blends of polystyrene (PS)–poly(2,6-dimethyl-1,4-phenylene oxide) (PPO) [16] and PS–poly(vinyl methyl ether) (PVME) [21,22]. Hubbell and Cooper [23] suggested that intrachain stiffness and the number of segments between crosslinks (entanglement density) are important factors in explaining segmental orientation for those blends that form a physical network.

Molecular orientation induced by uniaxial drawing of crystallizable miscible blends was studied by Keroack et al. [24] These blends were poly(ϵ-caprolactone) (PCL)–poly(vinyl chloride) (PVC) and PCL–poly(styrene-*co*-acrylonitrile) (SAN). The morphology resulting from the drawing process was suggested as being highly dependent on the initial blend crystallinity. For highly crystalline blends with volume-filling PCL spherulites, a very high segmental orientation of PCL was obtained in the crystalline domains. The drawing of these blends was found to result in the initial deformation of spherulites with subsequent transformation of lamellae into microfibrils upon further drawing. However, for PVC/PCL blends with 5% initial crystallinity,

* Corresponding author. Tel.: +1-330-972-6865; fax: +1-330-258-2339.
E-mail address: cakmak@uakron.edu (M. Cakmak).

0032-3861/02/$ - see front matter
PII: S0032-3861(01)00607-3

the high level of crystalline domains present in the PCL was suggested as being a result of microfibril-like crystallites of PCL formed by strain induced crystallization rather than the transformation of existing lamellae to the microfibrillar structure.

The ultimate goal of this study is to investigate the annealing behavior of pre-oriented PEEK/PEI blends that is the subject of the companion paper [25]. In order to better understand the heat setting at temperatures where the crystallization rates are typically fastest, a basic understanding of the initial structure of drawn PEEK/PEI blends is necessary. This paper includes a detailed study on the uniaxial constant width (UCW) deformation behavior of amorphous PEEK/PEI blends at 10°C above their respective glass transition temperatures. Beginning with an understanding of the deformation characteristics of neat PEEK, the focus is shifted to the effects associated with the addition of an amorphous component, PEI, and the analysis of changes in stress–strain behavior, due to orientation and strain-induced crystallization. The thermal behavior of the drawn blends with an emphasis placed on the glass transition (T_g) and cold crystallization (T_{cc}) is also investigated.

2. Experimental procedures

2.1. Preparation of the blends

Three compositions of PEEK/PEI blends were prepared: 90/10, 70/30, and 50/50 by weight. PEEK (Victrex 381G) (number average molecular weight $M_n \sim 15\,000$) and PEI (Ultem 1000) pellets were mechanically mixed and dried in the vacuum oven at 140°C for 24 h. Subsequent to drying, the pellets were melt mixed using 30 mm JSW co-rotating, intermeshing twin screw extruder with *L/D* (length to diameter) ratio of 32.5. The barrel temperature was set at 265°C for zone 1, 360°C for zone 2, and 380°C for zones 3–7 (zone number increases incrementally from the hopper towards the die). The temperature of the die was kept constant at 380°C. The extrudates were quenched in a water bath and pelletized.

2.2. Preparation of the films

The PEEK/PEI blends were melt cast using a Prodex one inch single screw extruder equipped with an eight inch wide sheet casting die and a take up system equipped with a temperature controlled quench roll. The melt temperature at the die was 400°C. The quench roll temperature was maintained at 98°C with the aid of a water circulating temperature control unit. The thickness of the film was controlled between 400 and 500 μm. The resulting films were all found to be amorphous by DSC study.

2.3. Thermal analysis

Thermal analysis of both the pelletized material and the cast film material was performed using a TA Instruments Thermal Analyst 3100 with DSC 2910 Differential Scanning Calorimeter. An indium standard was used to calibrate the temperature and heat flow.

For the accurate determination of the glass transition temperature for miscibility analysis, the samples were heated to 370°C at a heating rate of 50°C/min, kept isothermally at 370°C for 5 min and quenched in liquid nitrogen. These samples were then thermally scanned at a heating rate of 20°C/min. The glass transition temperature was analyzed at the inflection point of the transition.

Crystallinity of the films was calculated from DSC thermograms using the following equation

$$\text{Crystalinity}(\%) = \frac{\Delta H_{\text{exp}}}{\Delta H^0} \times 100 \tag{1}$$

where

$$\Delta H_{\text{exp}} = \Delta H_{\text{melting}} - \Delta H_{\text{coldcrystallization}} \tag{2}$$

where ΔH^0 is the heat of fusion for 100% crystalline polymer. The heat of fusion used for 100% crystalline PEEK was 130 J/g [26]. The crystallinity values were divided by the weight fraction of PEEK in order to normalize the crystallinity to the fraction of PEEK present in each blend.

2.4. Deformation behavior above the glass transition temperature

To study the effect of composition on the uniaxial deformation behavior, the cast films were drawn at 10°C above their T_gs using an Instron 4204 Tensile Tester equipped with an environmental oven. For this purpose, dumbbell-shaped samples having a 40 mm gauge length and 6 mm width were used. The oven was preheated for one hour at each processing temperature. After each of the samples was mounted on the grips, it was allowed to remain undisturbed in the oven for an additional 5 min, prior to drawing to allow for sample thermal equilibrium. The draw rate for the samples was 20%/s. True stress was calculated from the measured tensile force using the affine deformation assumption ($A \times L = A' \times L'$). After stretching to the preset ratio, the oven doors were opened and the sample was cooled with cold air with a fan and declamped after cooling to temperatures below its T_g, to eliminate possible relaxation.

2.5. Uniaxial constant width (UCW) drawing

Films with different draw ratios were prepared by an Iwamoto biaxial stretcher (BIX-702) at $T_g + 10$°C and with 20%/s draw rate. The UCW mode was used. The samples with dimensions of 12 cm × 12 cm were prepared and were marked at 2 cm intervals. The reported draw ratio reflects the local draw ratio measured between the marks. The samples were allowed to remain in the oven for 1–2 min prior to drawing, to allow the samples to attain thermal equilibrium. Prior to removing the samples from the

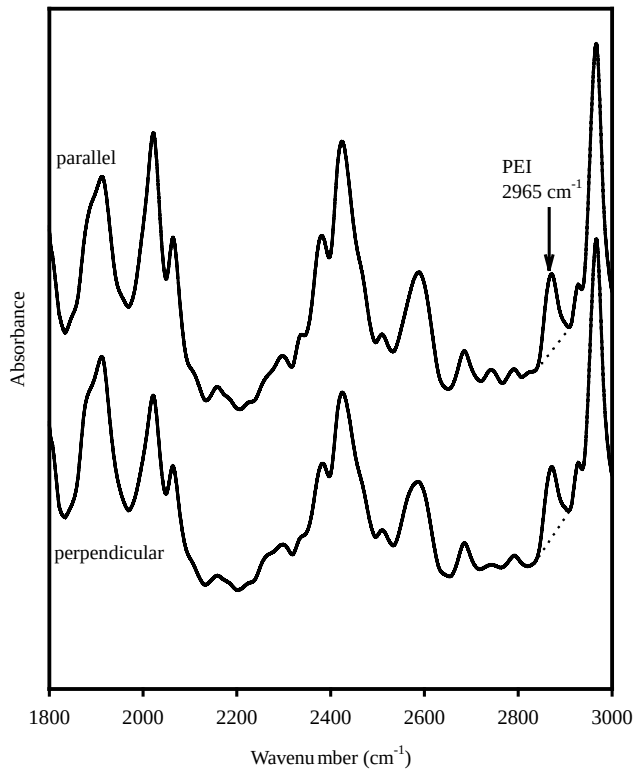

Fig. 1. Polarized infrared spectra of oriented PEEK/PEI (70/30) blend. The draw ratio is 3.

thermal chamber, the samples were rapidly cooled below the glass transition temperature using forced air.

2.6. Wide angle X-ray scattering (WAXS)

To study the structure evolution of the deformed films as a function of draw ratio and composition, wide angle X-ray scattering (WAXS) patterns on films of varying draw ratios were obtained using Rigaku 18 kW X-ray generator equipped with a Rigaku R-Axis image plate. The machine was operated at 50 kV and 250 mA. Cu Kα radiation ($\lambda = 1.542$ Å) was obtained using a Nickel foil filter. A beam collimator of 0.3 mm diameter was used. Sample to detector distance was set at 200 mm and the exposure time was set to 20–30 min.

2.7. Infrared dichroism

The preferential orientations of PEI in the drawn blend films were determined by infrared dichroism. The polarized spectra were recorded using a Nicolet 5SXC Fourier transform infrared (FTIR) spectrometer equipped with wire-grid polarizer and a TGS detector. All spectra were recorded at a resolution of 4 cm^{-1} (average of 64 interferograms). The IR dichroic ratio, D, was calculated as $D = A_{\parallel}/A_{\perp}$ with $A_{\parallel}$ and $A_{\perp}$ being the optical densities at the absorption maxima, measured parallel and perpendicular to the draw direction.

For the orientation of PEI, the band at 2965 cm^{-1} was used, which corresponds to the aliphatic C–H stretch. The drawn films were too thick for good quantitative IR analysis at wavenumbers below 2000 cm^{-1}; however, in the region of interest (between 2000 and 3000 cm^{-1}), the absorbance values were smaller than 1, thus allowing the application of Beer's law for analysis. An example of a typical spectrum and baseline determination is given in Fig. 1.

3. Results and discussion

3.1. Miscibility and thermal behavior of PEEK/PEI blends

DSC heating curves for amorphous PEEK/PEI blends are shown in Fig. 2. All the compositions have a single T_g. The T_gs of the blends in pellet forms and as-cast films are plotted as a function of blend composition in Fig. 3(a). It is observed that T_g of the blend increases at increasing concentrations of PEI and shows a negative deviation from linear dependency of T_g on the weight or volume fraction of the individual components. The negative deviation of T_g is generally attributed to the inrease in free volume, which often occurs in blends [27]. The compositional dependency of T_g gives the best fit by applying the Fox equation as shown by dotted line in Fig. 3(a). Fox equation is given as

$$\frac{1}{T_g} = \frac{w_1}{T_{g1}} + \frac{w_2}{T_{g2}} \tag{3}$$

where w_1 and w_2 represent the weight fractions of the blend constituents and T_{g1} and T_{g2} are their respective glass transition temperatures. The existence of a single T_g indicates that

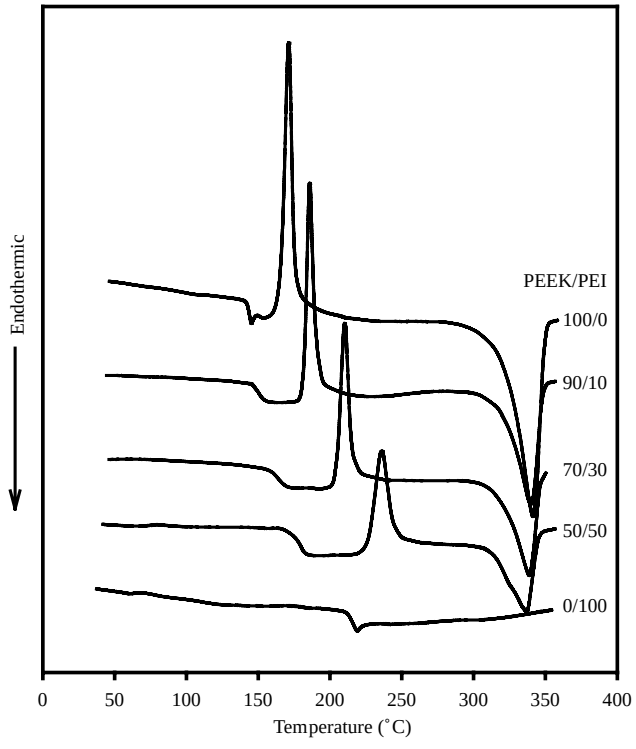

Fig. 2. DSC scans of amorphous PEEK/PEI blends. Heating rate: 20°C/min.

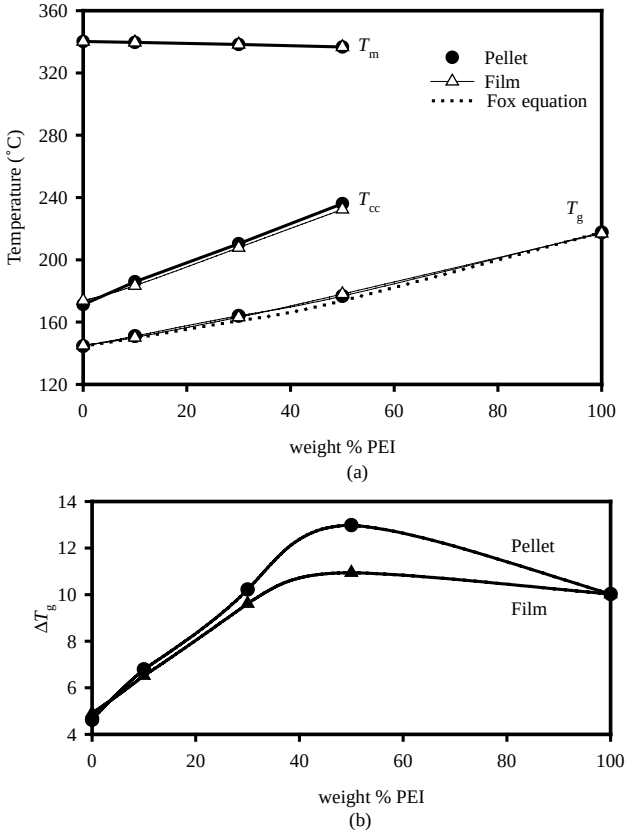

Fig. 3. The dependence of thermal properties of amorphous PEEK/PEI blends and cast-films of PEI concentration. (a) Glass transition (T_g), cold crystallization (T_{cc}), and melting (T_m) temperatures; (b) the width of T_g.

PEEK and PEI are miscible in the amorphous state. This is consistent with the conclusions of miscibility studies carried out by other researchers [4,12]. The miscibility of these polymers was attributed to the favorable interactions that take place between the oxygen ion-pair electrons of the ether group in PEEK and electron-deficient imide rings in PEI [28].

The dependence of the width of the T_g transition (ΔT_g) on composition is shown in Fig. 3(b). ΔT_g has previously been used to evaluate the miscibility for blends. Fried et al. [29] suggested that ΔT_g is approximately 10°C for miscible blends. The increase in the width of the T_g transition range is generally attributed to increased local composition fluctuations [30]. For the pellet and cast amorphous films, there appears to be a maximum ΔT_g at mid-concentrations of PEEK and PEI; however, the overall width of this transitional area is relatively small. Consequently, since the T_g and ΔT_g of the cast films are identical to those of the amorphous pellets, it can be concluded that little or no phase separation has occurred during the film quenching process.

At temperatures above T_g, PEEK begins to crystallize at 170°C and the melting begins to occur at 310°C. Upon the addition of increasing amounts of PEI, the cold crystallization temperature of PEEK moves to higher temperatures. This result is due to the dilution of PEEK crystals by noncrystallizable PEI chains. It is expected that the addition of a noncrystallizing polymer to a crystallizable polymer reduces the crystallization rate of the blend. This is attributed to a reduction in the mole ratio of the crystallizing species available for crystallization, reduction in thermodynamic driving force and reduction in transport rate of chains of the crystallizing species across the growth front. The increase in width to height ratio of the melting peak attributed to PEEK indicates that there is a detrimental change in the perfect crystalline domains, characteristic of pure PEEK with the inclusion of increasing amounts of PEI (Fig. 2). It is also observed that the melting temperature of PEEK has slightly decreased with the addition of PEI. Hsiao and Sauer [11] found a similar type behavior for their blend systems.

3.2. Uniaxial deformation behavior of PEEK/PEI films in the rubbery region

3.2.1. Stress–strain curves at T_g + 10°C

In a tenter-frame process, the thermoplastic films are drawn above their T_g, where the chains have adequate molecular mobility but sufficiently below T_{cc} to prevent thermally induced crystallization during the course of deformation. The temperature range T_{cc}–T_g defines the processing window for these films and this value is approximately 28°C for pure PEEK. This processing window is relatively small when compared to other polymers; e.g. PET (125 − 70 = 55°C), PEN (190 − 120 = 70°C). This window is enlarged with the addition of noncrystallizable PEI as indicated in Fig. 3(a). For pure PEEK, there is always a danger of rapid thermal nucleation coupled with the growth of large crystals that have the propensity to affect the transparency of the film and prematurely halt the deformation. As a side benefit, blending amorphous PEI with PEEK reduces the size of crystals and consequently leads to films with enhanced transparency.

To study the effect of composition on the deformation behavior, blend films at different compositional ratios of PEEK and PEI were brought to a comparable thermal state by drawing them at 10°C above their respective T_gs. They were subsequently cooled to room temperature by forced room temperature air blowing on to the samples while they are clamped. Fig. 4 shows the stress–strain curves of PEEK/PEI blends drawn at T_g + 10°C with a constant extension rate of 20%/s in the UFW mode. Because of the T_g broadening, the drawing temperature becomes closer to the T_g region as the concentration of the PEI is increased. Despite this effect, the drawing temperature remains outside the T_g region for all compositions studied. Evaluation of these stress–strain curves shows that higher compositional levels of PEI exhibit higher stresses during the initial stages of deformation up to a draw ratio of 2.8; however, additional deformation results in lower stresses for the higher PEI concentrations.

As will be explained in Section 3.3, during the initial

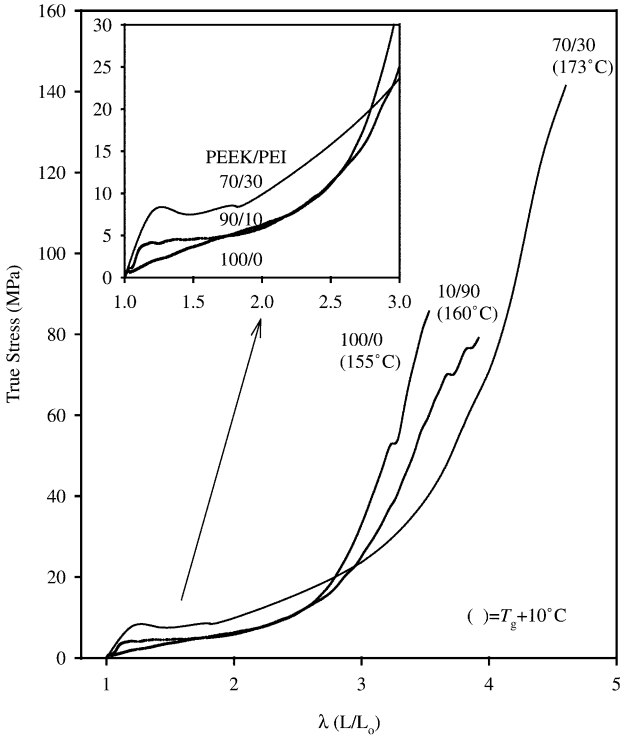

Fig. 4. True stress versus draw ratio for PEEK/PEI films drawn at T_g + 10°C and with 20%/s.

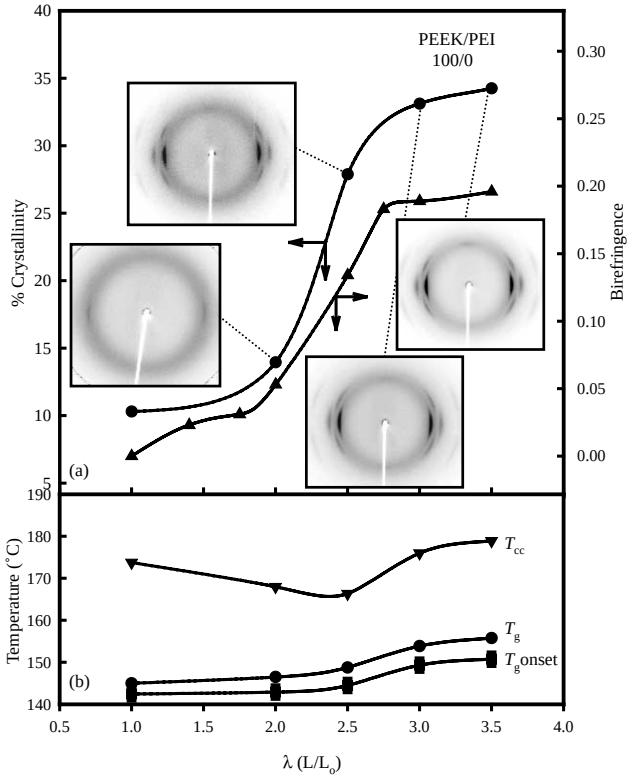

Fig. 5. Properties of PEEK films drawn at 155°C (T_g + 10°C) at different draw ratios. (a) WAXD patterns, crystallinity, and birefringence profile; (b) glass transition temperature (T_g) and clod crystallization temperature (T_{cc}).

stages of deformation, the blends possess low levels of crystallinity. The increased stresses at high levels of PEI during the initial stages of deformation are due to greater internal molecular friction forces generated in the presence of stiff and bulky PEI chains that move past one another. Conversely, in the later stages of deformation and at high levels of PEEK, strain hardening is observed which results from the strain-induced crystallization of PEEK. For neat PEEK, stress levels increase sharply above a draw ratio of approximately 2.5 (Fig. 4). In addition, for high levels of PEI, the onset of strain induced crystallization with respect to deformation is delayed to a draw ratio greater than 3 due to an increase of amorphous component concentration. It was also observed that the 'stretchability' of the PEEK/PEI films was improved with the addition of PEI as a result of its suppression of strain hardening.

3.3. Crystallinity and orientation development in drawn films

In order to understand the structure development during uniaxial drawing of PEEK/PEI films above their glass transition temperatures, films at different draw ratios were prepared and the drawn films were analyzed using DSC, WAXD, spectral birefringence and IR dichroism.

The uniaxial deformation behavior of PEEK was analyzed and is shown in Fig. 4. Below a draw ratio of approximately 2, PEEK films exhibit low birefringence and crystallinity levels. These birefringence and crystallinity values agree quite well with the ones found by Bassigny et al. [31], who studied the tensile drawing of PEEK using birefringence, infrared dichroism and shrinkage–stress measurements. Fig. 5 shows a dramatic increase in the birefringence at low strains followed by a pseudo plateau region where birefringence remains relatively constant with draw ratio. This plateau region can be explained as molecular chains slipping past one another in the absence of a well-defined physical network. To support the concept of the lack of a highly structured physical network, one should consider the fact that PEEK has relatively low molecular weight (number average molecular weight $M_n \sim 15\,000$) and an average of only three entanglements per chain [31].

During the second stage of deformation (beyond an approximate draw ratio of 2), a sudden and sharp increase in crystallinity and birefringence levels are observed. The draw ratio (2.0) corresponding to the increase in birefringence and crystallinity correlates well with the draw ratio (2.5) at the onset of strain hardening observed in the stress–strain curve of neat PEEK (Fig. 4) if consideration is given to the different modes of deformation. The samples drawn in UCW mode (birefringence, crystallinity determinations) can be expected to have a lower draw ratio for the onset of strain hardening compared to the samples drawn in UFW mode (stress–strain curves). Noting that thermally induced

crystallization for PEEK does not occur at 155°C within the time frame of drawing, the development of crystallinity during strain hardening must be entirely due to strain-induced crystallization of highly extended chains. The studies done by Chien and Weiss [32] on the strain-induced crystallization behavior of PEEK shows that, under conditions where no quiescent crystallization occurs, the activation energy for crystallization is greatly reduced as a result of chain orientation. WAXD patterns indicate that upon stretching to a stretch ratio 2, a sharp equatorial peak emerges at the approximate peak location of first amorphous halo that corresponds to interchain correlations. This peak is eventually identified as (110) crystalline peak upon establishment of three-dimensional lattice at higher stretch ratios/crystallinities. The WAXD pattern of the drawn film at $\lambda = 2$, shows a very sharp peak with a small azimuthal spread at the equator but does not show any off-equatorial peaks. This indicates that there are highly oriented crystalline regions but the chains do not have adequate registry with each other along the *c*-axis to establish a full three-dimensional ordered lattice structure. Upon stretching further, the three dimensional order is established by the clear appearance of equatorial (200) and first layer line (113) peaks.

The sharp increase in stresses as a result of strain-induced crystallization of highly extended chains suggests that this stage of deformation can be characterized by the formation of a physical network. This network is considered to consist of nodes formed by highly oriented crystallites that carry the applied stress thus preventing chain slippage. As a result of the formation of this network, the deformation process leads to chain extension, thus increasing the overall birefringence of the material. The formation of this physical network was also proven by the draw ratio dependence of the axial Young's modulus and thermal expansion behavior of PEEK studied by Choy et al. [33]. The axial modulus was found to vary little with draw ratio below the onset of strain hardening and increase rapidly upon further drawing. The strong increase in the modulus was related to the presence of highly aligned tie molecules in the amorphous region connecting the crystallites, which act as physical cross-links. The existence of taut tie molecules is evidenced by the decrease of axial thermal expansion coefficient with increase in draw ratio over a given temperature range. Additionally, when tie chains are present, the transverse thermal expansion increases with draw ratio.

At the last stages of deformation, it is observed that crystallinity, birefringence and orientation show little increase with draw ratio and further drawing eventually leads to the breakage of the films.

Fig. 5(b) shows the thermal behavior of drawn PEEK films. The cold crystallization decreases and the T_g increases slightly with draw ratio up to a draw ratio of 2.5. The decrease in T_{cc} can be explained by the decrease in the entropy of the polymer chains as a result of preferential orientation under deformation and an increase in the driving force for crystallization; therefore, crystallization takes

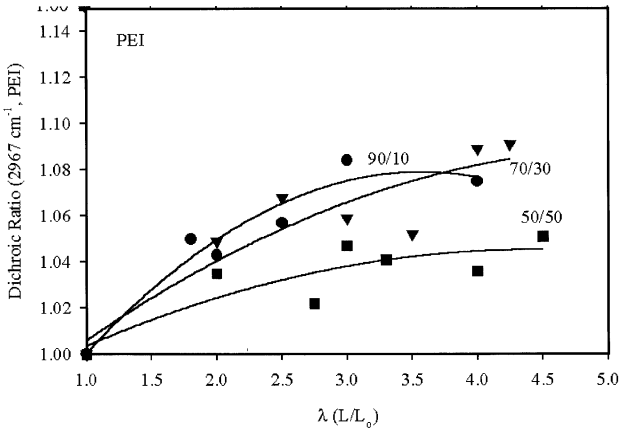

Fig. 6. The variation of orientation OF PEI with draw ratio and with composition in drawn PEEK/PEI blends.

place at lower temperatures as evidenced by DSC. On the other hand, the increase in crystalline domains in the system restricts the molecular mobility in the amorphous domains and as a result, T_g is increased. The increase in T_g becomes more evident at high draw ratios where the crystallinity levels are much higher; for example at $\lambda = 3.5$, T_g is increased by almost 10°C. The increase in T_{cc} on materials with a draw ratio of 2.5 or greater is a direct consequence of the increase of T_g, decreased chain mobility and a reduction

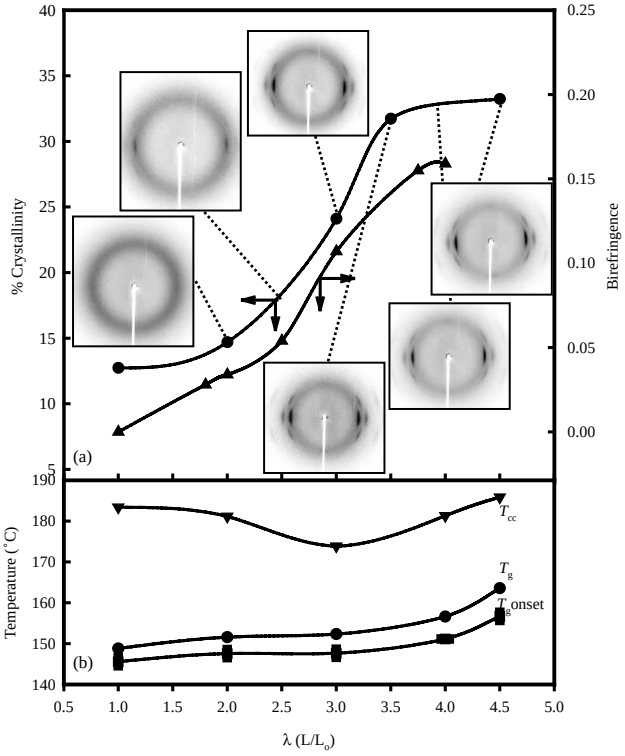

Fig. 7. Properties of PEEK/PEI (90/10) films stretched at 160°C (T_g + 10°C) at different draw ratios. (a) WAXD patterns, crystallinity, and birefingence profile; (b) glass transition temperature (T_g) and cold crystallization temperature (T_{cc}).

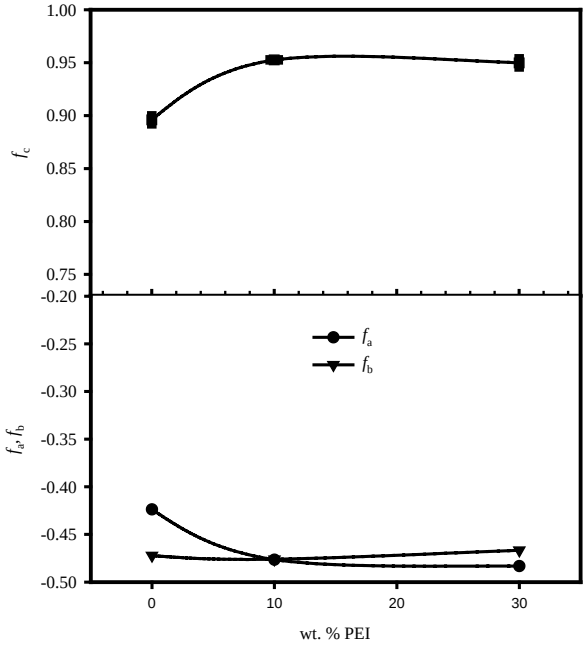

Fig. 8. The variation of *a*, *b* and *c* axes orientations of PEEK crystal with PEI concentration in 3 × drawn PEEK/PEI films.

in the crystallization rate. WAXD patterns and birefringence data indicate that above $\lambda = 3.0$–3.5, orientation and crystallinity do not change significantly with drawing; thus the T_{cc} and T_g show little change with draw ratios above 3.0–3.5.

Fig. 6 describes the orientation behavior of PEI chains at various compositions and draw ratios. It is observed that PEI chain orientations are lowered with increasing PEI concentrations and are increased with draw ratio.

Figs. 7–10 describe the thermal behavior, crystallinity and birefringence development in PEEK/PEI films. For the 90/10 blend, birefringence and crystallinity levels of PEEK are slightly decreased compared to neat PEEK as shown in Fig. 7 and the behavior of T_{cc} and T_g with draw ratio is very similar to what was observed in pure PEEK. The increase in T_g with drawing may be affected by the enrichment of PEI domains by their expulsion from crystallizing PEEK domains. When Chen and Porter [34] studied uniaxial draw of amorphous PEEK/PEI blends at 125°C, they observed a decrease in T_g with draw ratio over the whole composition range. They postulated that the depression of T_g as a result of cold drawing of PEEK/PEI blends might be related to the alteration of the segmental packing,

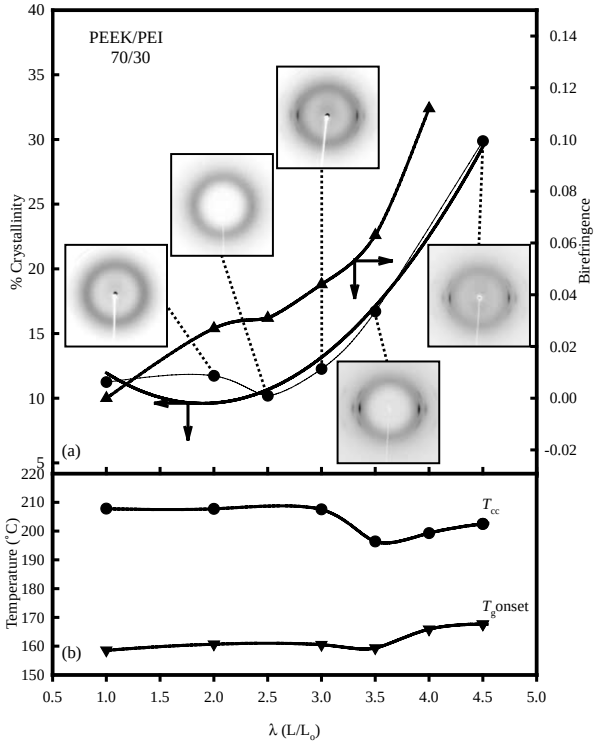

Fig. 9. Properties of PEEK/PEI (70/30) films drawn at 173°C (T_g + 10°C) at different draw ratios. (a) WAXD patterns, crystallinity, and birefringence profile; (b) glass transition temperature (T_g) and cold crystallization temperature (T_{cc}).

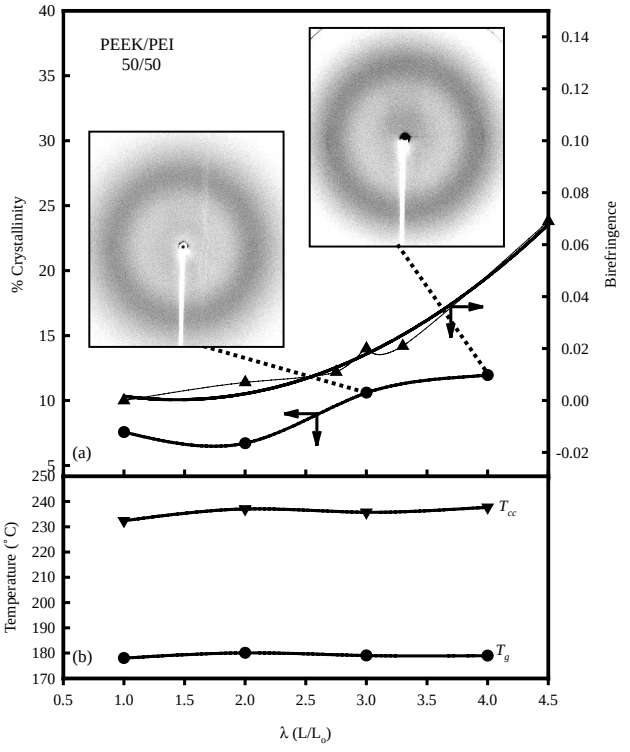

Fig. 10. Properties of PEEK/PEI (50/50) films drawn at 188°C (T_g + 10°C) at different draw ratios. (a) WAXD patterns, crystallinity, and birefringence profile ;(b) glass transition temperature (T_g) and cold crystallization (T_{cc}) temperature.

the chain conformation and the distribution of free volume. As indicated by Fig. 7, the strain-induced crystallization and the increase of order in the crystalline domains in PEEK/PEI blends are delayed to higher draw ratios. Even though the overall orientation of PEEK is decreased with the addition of PEI, as revealed by reduced birefringence levels, WAXD patterns show very sharp and oriented PEEK crystals. The azimuthal spread of these diffraction peaks is smaller than the ones observed in WAXD patterns of pure PEEK, indicating a higher orientation. The orientation levels of PEEK crystals for drawn films ($\lambda = 3$) were quantified as shown in Fig. 8. The orientation factors of a, b and c axes of PEEK crystals were calculated by the procedure presented in the companion paper [25]. In this procedure, a careful removal of contributions from the anisotropic amorphous background was undertaken to remove their effect. The c-axis orientation levels are very high, close to the theoretical limit of 1; and, a and b axes orientations are very close to -0.5 (Fig. 8). These values indicate that the chains in the crystalline regions are almost parallel with the draw direction. The orientation values are much higher than the ones reported by Lee et al. [35] because they failed to subtract the anisotropic amorphous background azimuthal intensity profile from the crystalline diffraction intensity profile. This results in significant underestimation of crystalline orientations. Fig. 8 shows that the chain axis orientation of the PEEK crystals increases with the increase in PEI concentration. The highly oriented structure of PEEK crystals is preserved even in blends with 30 wt% PEI, as illustrated in Fig. 9. This shows that although the crystallization of PEEK is retarded because of the dilution effect of PEI, PEEK in the blends crystallizes the same way as in the pure state. This behavior was also observed in the quiescent crystallization of PEEK/PEI blends in the melt or in the rubbery state [4,10,11]. With further increase in PEI to 30 and 50 wt% concentration, the crystallinity levels are significantly lowered (Figs. 9 and 10). The films with 50 wt% PEI, do not show any crystalline order unless substantial deformation levels are imparted on these films. The first sign of oriented crystal formation is observed in WAXD patterns at draw ratios of $\lambda = 4$, where we begin seeing the diffraction of the (110) plane (Fig. 10). At this level of PEI concentration, the cold crystallization temperature and the glass transition temperature do not change significantly with the draw ratios used in this study.

4. Conclusions

The deformation behavior of PEEK/PEI blends with PEEK concentration higher than 50 wt% is schematically illustrated in Fig. 11. When PEEK/PEI blends are drawn in their rubbery region, prior to the critical draw ratio (onset of strain hardening), they exhibit lower stress values (Fig. 11(b)). In the initial stages of deformation, the films

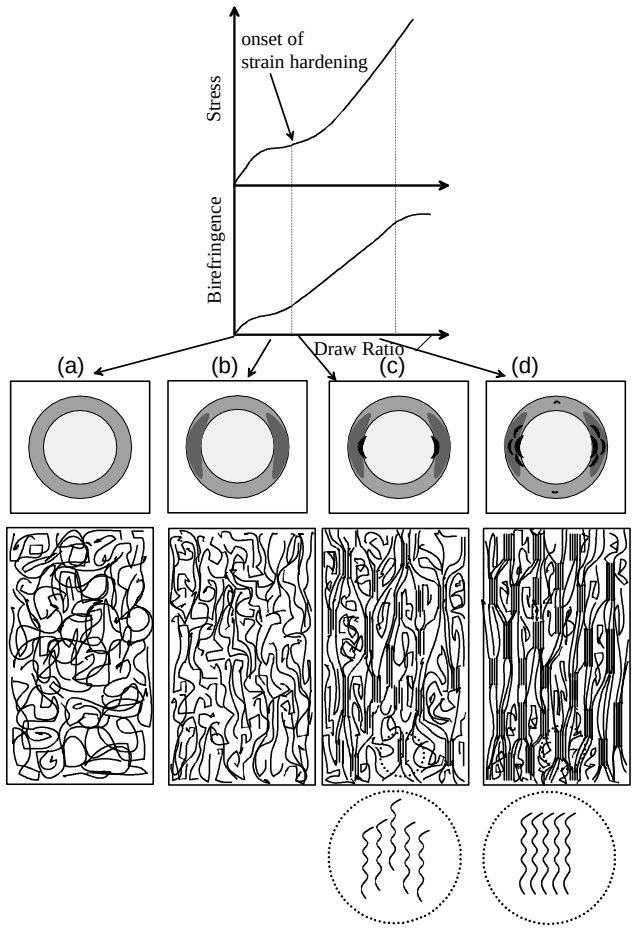

Fig. 11. Schematic illustration of the uniaxial deformation behavior of PEEK/PEI blends with PEEK content higher than 50 wt%. a, b, c and d describe different stages of drawing with increasing draw raito.

are amorphous and upon stretching gradually oriented as detected by IR dichroism and birefringence. Subsequent to the onset of strain hardening, the stress rises rapidly because of strain-induced crystallization of the chains highly oriented in the direction of strain. It is during this stage of deformation process that *a highly structured physical network is formed where oriented crystallites act as nodes in the network structure*. As is evidenced by the sharp equatorial interchain correlation peak, there are regions that exhibit near perfect orientation of polymer chains along the stretching direction but exhibit high axial displacement disorder (Fig. 11c). As a result, off-equatorial peaks are not observed at early stages of deformation. Once these highly oriented nodes are formed, the order in the crystalline domains increases very rapidly with draw ratio (Fig. 11(d)). During this period, the effectiveness of drawing arises from the existence of the tie chains aligned in the direction of draw and forming the net between the crystallites. PEI is found to delay the oriented crystallization rate of PEEK, but has little effect on its crystalline orientation. PEI chains are also oriented with drawing. The overall chain orientation in PEEK is increased as a result of blending with PEI. Drawing

was found to significantly increase the T_g of the blends, as much as 10°C for the case of pure PEEK at $\lambda = 3.5$.

References

[1] Cakmak M. Polyaryl ether ketones: properties and structure development. In: Olabisi O, editor. Handbook of thermoplastics. New York: Marcel Dekker, 1999.
[2] Harris JE, Robeson LM. J Appl Polym Sci 1988;35:1877.
[3] Barlow JW, Paul DR. Polym Engng Sci 1987;27:1482.
[4] Crevecoeur G, Groeninckx G. Macromolecules 1991;24:1190.
[5] Bristow JF, Kalika DS. Polymer 1997;38:287.
[6] Chen H-L, Porter RS. Polym Engng Sci 1992;32:1870.
[7] Jonas AM, Ivanov DA, Yoon DY. Macromolecules 1998;31:5352.
[8] Chen H-L, Porter RS. J Polym Sci, Polym Phys 1993;31:1845.
[9] Chen H-L, You J-W, Porter RS. J Polym Res 1996;3:151.
[10] Hudson SD, Davis DD, Lovinger AJ. Macromolecules 1992;25:1759.
[11] Hsiao BS, Sauer BB. J Polym Sci, Polym Phys Ed 1993;31:901.
[12] Harris JE, Robeson LM. J Polym Sci, Polym Phys Ed 1987;25:311.
[13] Hsiao BJ, Verma RK, Sauer BB. J Macromol Sci, Phys 1998; B37(3):365.
[14] Ivanov DA, Jonas AM. Macromolecules 1998;31:4546.
[15] Ivanov DA, Lipnik PDM, Jonas AM. J Polym Sci, Polym Phys 1997;35:2565.
[16] Lefebvre D, Jasse B, Monnerie L. Polymer 1984;25:318.
[17] Zhao Y, Jasse B, Monnerie L. Polymer 1989;30:1643.
[18] Chabot P, Prud'homme RE, Pezolet M. J Polym Sci, Polym Phys 1990;28:1283.
[19] Kamura M, Tabuse H, Kuramoto N. Japan Patent 631 4934 A2 [8814934], 1988.
[20] Zhao Y, Prud'homme RE, Bazuin CG. Macromolecules 1991;24: 1261.
[21] Hoffmann U, Klapner M, Mullen K. Polym Bull 1993;30:481.
[22] Faivre JP, Jasse B, Monnerie L. Polymer 1985;26:879.
[23] Hubbell DS, Cooper SL. J Polym Sci, Polym Phys 1977;15:1143.
[24] Keroack D, Zhao Y, Prud'homme RE. Polymer 1998;40:243.
[25] Bicakci S, Cakmak M. Polymer (submitted).
[26] Blundell DJ, Osborn BN. Polymer 1983;24:953.
[27] Brekner J-M, Schneider HA, Cantow H-J. Polymer 1988;29:78.
[28] Chen H-L, You J-W, Porter RS. J Polym Res 1996;3:151.
[29] Fried JR, Karasz FE, McKnight WJ. Macromolecules 1978;11:150.
[30] Galin M. Makromol Chem 1987;188:1391.
[31] Bassigny V, Séguéla R, Rietsch F, Jasse B. Polymer 1993;34:4052.
[32] Chien MC, Weiss RA. Polym Engng Sci 1988;28:6.
[33] Choy CL, Leung WP, Nakafuku C. J Polym Sci, Polym Phys 1990;28: 1965.
[34] Chen H-L, Porter RS. Macromolecules 1995;28:3918.
[35] Lee Y, Lefebvre J-M, Porter RS. J Polym Sci, Polym Phys 1988; 26:795.